

INDIRECT DETECTION OF CMSSM NEUTRALINO DARK MATTER WITH NEUTRINO TELESCOPES

J. ORLOFF* AND E. NEZRI

*Laboratoire de Physique Corpusculaire,
IN2P3-CNRS, Université Blaise Pascal, F-63177 Aubièrre Cedex
E-mail: orloff@in2p3.fr, nezri@in2p3.fr*

V. BERTIN

*Centre de Physique des Particules de Marseille,
IN2P3-CNRS, Université de la Méditerranée, F-13288 Marseille Cedex 09
E-mail: bertin@in2p3.fr*

We review the prospects of detecting supersymmetric dark matter in the framework of the Constrained Minimal Supersymmetric Standard Model, and compare indirect with direct detection capabilities.

Recently, both theoretical considerations and a wealth of experimental data in cosmology have converged towards a Λ CDM flat and black universe, with the following amounts of dark energy and cold dark matter: $\Omega_\Lambda \sim 0.7$, $\Omega_{CDM} \sim 0.3$. This last fraction could be incarnated by a bath of Weakly Interacting Massive Particles (WIMPs), whose annihilation stopped when the universe expansion separated them enough from each other, leaving a non relativistic relic density. In the MSSM framework, assuming R-parity conservation, the Lightest Supersymmetric Particle (LSP) is stable and is the lightest neutralino (\doteq the neutralino(s) χ) in most regions of the parameter space. If present in galactic halos, relic neutralinos must accumulate in astrophysical bodies (of mass M_b) like the Earth or most importantly the Sun¹, which then play the role of cosmic storage rings for neutralinos. The capture rate C depends on the neutralino-quark elastic cross section: $\sigma_{\chi-q}$. Neutralinos being Majorana particles, their vectorial interaction vanishes and the allowed interactions are scalar (via

*presented by J. Orloff

$\chi q \xrightarrow{H\bar{q}} \chi q$ in t channel and $\chi q \xrightarrow{\bar{q}} \chi q$ in s channel) and axial (via $\chi q \xrightarrow{Z} \chi q$ in t channel and $\chi q \xrightarrow{\bar{q}} \chi q$ in s channel). Depending on the spin content of the nuclei N present in the body, scalar and/or axial interactions are involved. Roughly, $C \sim \frac{\rho_\chi}{v_\chi} \sum_N M_b f_N \frac{\sigma_N}{m_\chi m_N} \langle v_{esc}^2 \rangle_N F(v_\chi, v_{esc}, m_\chi, m_N)$, where ρ_χ, v_χ are the local neutralino density and velocity, f_N is the density of nucleus N in the body, σ_N the nucleus-neutralino elastic cross section, v_{esc} the escape velocity and F a suppression factor depending on masses and velocity mismatching. Considering that the population of captured neutralinos has a velocity lower than the escape velocity, and therefore neglecting evaporation, the total number N_χ of neutralinos in a massive astrophysical object depends on the balance between capture and annihilation rates: $\dot{N}_\chi = C - C_A N_\chi^2$, where C_A is the total annihilation cross section $\sigma_{\chi-\chi}^A$ times the relative velocity divided by the volume. The annihilation rate at a given time t is then:

$$\Gamma_A = \frac{1}{2} C_A N_\chi^2 = \frac{C}{2} \tanh^2(t\sqrt{CC_A}) \quad (1)$$

with $\Gamma_A \approx \frac{C}{2} = cste$ when the neutralino population has reached equilibrium, and $\Gamma_A \approx \frac{1}{2} C^2 C_A t^2$ in the initial collection period (relevant in the Earth). So, when accretion is efficient, the annihilation rate does not depend on annihilation processes but follows the capture rate C and thus the neutralino-quark elastic cross section. The neutrino differential flux resulting from $\chi\chi$ annihilation is given by:

$$\frac{d\Phi}{dE} = \frac{\Gamma_A}{4\pi R^2} \sum_F B_F \left(\frac{dN}{dE} \right)_F \quad (2)$$

where R is the distance between the source and the detector, B_F is the branching ratio of annihilation channel F and $(dN/dE)_F$ its differential neutrino spectrum. As the direct neutrino production $\chi\chi \rightarrow \nu\bar{\nu}$ exactly vanishes in the massless neutrino limit, neutrino fluxes mainly come from decays of primary annihilation products, with a mean energy $E_\nu \sim \frac{m_\chi}{2}$ to $\frac{m_\chi}{3}$ (see figure 1). The most energetic “hard” spectra come from neutralino annihilations into WW or ZZ , and the less energetic “soft” ones come from $b\bar{b}$. Neutrino telescopes use the Earth as a target for converting the muon component of these neutrino fluxes into measurable muons (see S. Cartwright, these proceedings). As both the ν_μ charged-current cross section on Earth nuclei and the produced muon range are proportional to E_ν , high energy neutrinos are easier to detect.

The branching fractions B_F are thus relevant neutralino properties that depend on the particular SUSY model considered. We² have studied these

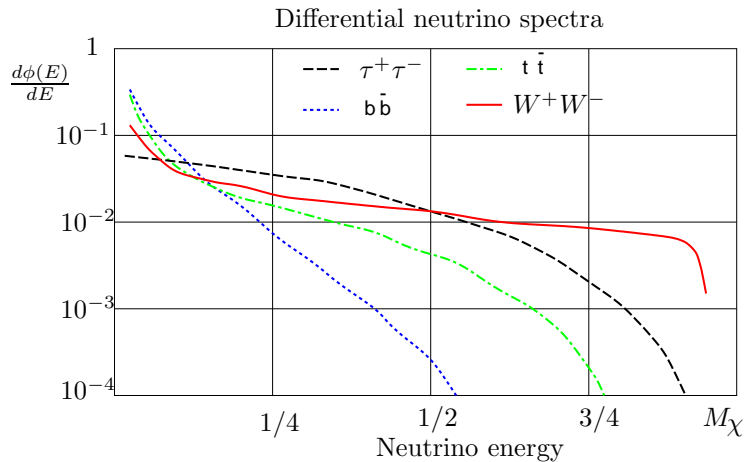


Figure 1. Energy dependence of secondary neutrino fluxes (in arbitrary units) from dominant neutralino annihilation channels, as functions of the neutrino energy in units of the neutralino mass.

in the Constrained Minimal Supersymmetric Standard Model (CMSSM, *a.k.a.* mSUGRA), whose attractiveness comes from a tractable number of free parameters: m_0 (common scalar mass), $m_{1/2}$ (common gaugino mass), A_0 (common trilinear term) and $sign(\mu)$ (supersymmetric scalar mass term), all fixed at a high energy scale $E_{GUT} \sim 2.10^{16}$ GeV, as well as $\tan\beta$, fixed at the EW scale. The coexistence of these widely different scales introduces theoretical uncertainties on the exact definition of the model (especially at large $\tan\beta$), but the advent of more and more reliable Renormalization Group Equations codes (like `Suspect2.005`³ used in this work) tends to reduce these. As a bonus, coping with RGE's from the start guarantees the expandability of the model to high energies which is the main motivation for introducing SUSY and neutralinos in the first place.

As seen on figure 2, the hard spectra from W^+W^- and $t\bar{t}$, are found at large m_0 for fixed $m_{1/2}$ larger than the corresponding threshold. In this “focus point” region⁴, the neutralino has a sizeable higgsino component $h_{frac}(\chi^0)$ which allows its annihilation into gauge bosons via t -channel gaugino exchange, with a cross-section $\sigma_A \propto h_{frac}^2(\chi^0)h_{frac}^2(\chi^+)$ and an interesting relic density may survive. Although this region seems a small fine-tuned corner of the $(m_0, m_{1/2})$ plane, relaxing universality may help in this respect^{5,6} Otherwise, the neutralino is an almost pure bino mainly annihilating into $b\bar{b}$ through s -channel A exchange or t -channel sfermion

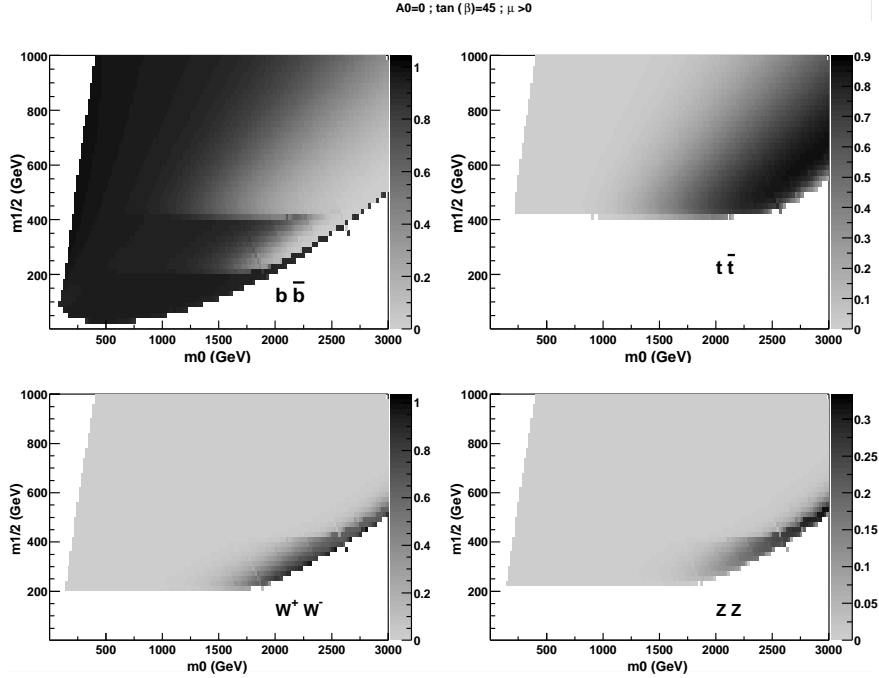


Figure 2. The dominant neutralino annihilation branching ratios for a typical large $\tan\beta = 45$ case, as functions of m_0 (common scalar mass) and $m_{1/2}$ (common gaugino mass).

exchange; a low enough relic density can only be found at small m_0 for fixed but not too large $m_{1/2}$.

To study the detectability of mSugra dark matter, we have used the `DarkSusy`⁷ code and computed 1) the relic density, 2) the solar muon flux seen by neutrino telescopes and 3) the scalar elastic cross section $\sigma_{\chi-p}^{scal}$ relevant to Germanium or Xenon direct detection, for a wide range of such mSugra models: $m_{1/2} \in (50, 1000)$ GeV, $m_0 \in (0, 3000)$ GeV, $\tan\beta = 10, 20, 35, 45, 50$, $\mu > 0$, $A_0 = -800, -400, 0, 400, 800$ GeV (for $\tan\beta = 20, 35$ only). Among these, we kept only those satisfying the following accelerator constraints: $BR(b \rightarrow s\gamma) \in (2.2, 5.2) \times 10^{-4}$, $a_\mu^{susy} \in (-6, 58) \times 10^{-10}$, $m_{\chi_1^+} > 104$ GeV, $m_h > 113$ GeV.

In left figure 3, these models are sorted according to their neutralino mass and the muon flux Φ_μ above 5GeV originating from the Sun. This is compared with past and future experimental sensitivities assuming the hardest neutrino spectrum of figure 1 normalized to Φ_μ : the lower threshold

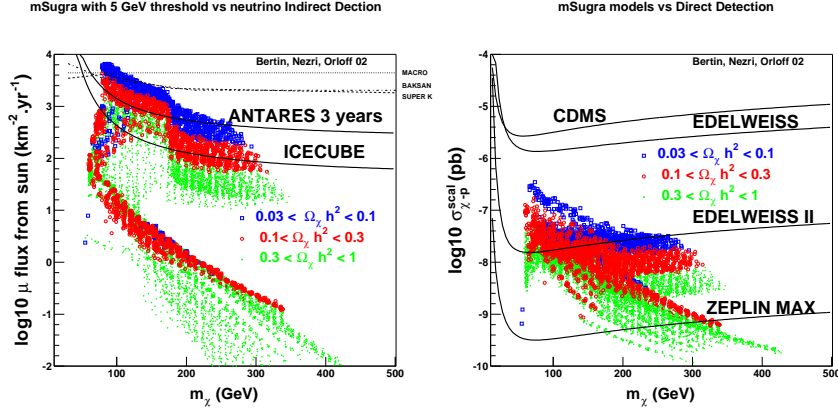


Figure 3. Indirect (left) and direct (right) detection potential of present and future experiments for mSugra models satisfying present experimental limits and offering interesting relic densities.

of Baksan or SuperK thus show as a better sensitivity at low m_χ . Applying the shown cuts on the relic density^a separates the models in the 2 rough classes indicated above: the lower half corresponds to binos, while the upper half is populated by models in the “focus point” region and neutralinos with a sizeable $h_{frac}(\chi)$. In this region, one clearly notices the W^+W^- and $t\bar{t}$ thresholds at $m_\chi = 89$ and 175 GeV respectively. Between these, the neutrino spectrum is indeed hard, and we see that Antares has the potential of detecting the models with the expected relic density $\Omega = 0.3$. For fixed m_χ , one also notices the correlation $\Phi_\mu \propto (\Omega h^2)^{-1}$, which can be understood as both the annihilation amplitude (determining the relic density) and the spin dependent collision amplitude (determining the capture in the Sun and thus the muon flux) are $\propto h_{frac}^2(\chi)$. When the mSugra neutralino is a bino, its spin dependent capture in the Sun is much reduced and the muon flux is far below present or future detection abilities. Similarly, neutralinos captured and annihilating in the Earth give far too low fluxes for mSugra models.

Turning to direct detection, the right figure 3 shows that for small masses, both the bino and focus region neutralinos are within reach of the next generation of direct detection experiments like Edeweiss II. The smaller vertical spread can be traced to the fact that the spin independent (or scalar) collision amplitude is proportional to only one power of $h_{frac}(\chi)$,

^aThe dimensionless Hubble parameter squared h^2 is about 0.5

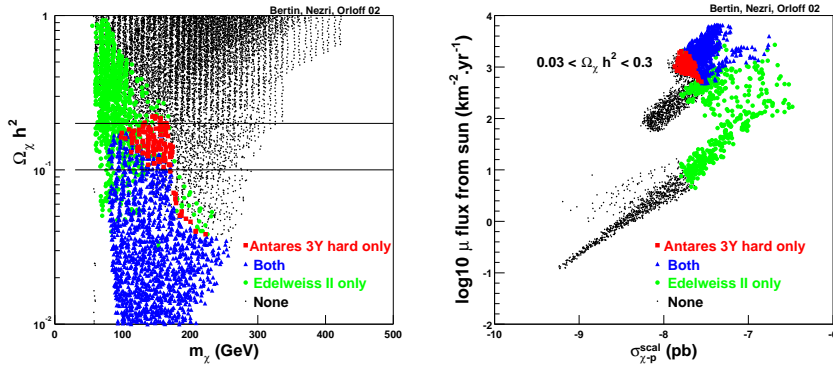


Figure 4. Other projections of the same mSugra models as in fig 3: left in the $(m_\chi, \Omega h^2)$ plane; right in the $(\sigma_{\chi-p}^{\text{scalar}}, \Phi_\mu)$ plane for $\Omega h^2 \in (0.03, 0.3)$. Each model is labelled according to its detectability: by Antares only, by Edelweiss II only, by both or none.

which results in a much weaker increase in the focus region. Also notice that an ultimate direct detection tool like Zeplin in a maximal version seems to cover all interesting relic densities. However coannihilations with staus (not included here) can allow for larger masses which would still be out of reach.

Another way to compare the merits of (in)direct detectors of mSugra dark matter is shown on figure 4. On the left, all mSugra models of the set defined above are placed in the $(m_\chi, \Omega h^2)$ plane and sorted by their detectability. On the right, the models with a relic density $\Omega h^2 \in [0.03, 0.3]$ are placed in the $(\sigma_{\chi-p}^{\text{scalar}}, \Phi_\mu)$ plane and sorted the same. Notice again the split in 2 groups, the upper half one again being the mixed neutralinos of the focus region. A complementarity between direct and indirect detection emerges from this splitting.

References

1. G. Jungman, M. Kamionkowski, and K. Griest. *Phys. Rept.*, 267:195–373, 1996.
2. V. Bertin, E. Nezri, and J. Orloff. *Eur. Phys. J.*, C26:111–124, 2002.
3. A. Djouadi, J.L. Kneur, and G. Moultaka. hep-ph/0211331.
4. J. L. Feng, K. T. Matchev, and F. Wilczek. *Phys. Lett.*, B482:388–399, 2000.
5. V. Bertin, E. Nezri, and J. Orloff. hep-ph/0210034.
6. J. R. Ellis, Keith A. Olive, and Yudi Santoso. *Phys. Lett.*, B539:107–118, 2002.
7. P. Gondolo, J. Edsjo, L. Bergstrom, P. Ullio, and T. Baltz. Darksusy program, <http://www.physto.se/~edsjo/darksusy/>.